STEM CELLS AND DEVELOPMENT
Volume 22, Number 23, 2013

DOI: 10.1089/scd.2013.0073

In Vivo Identity of Tendon Stem Cells and the Roles of Stem Cells in Tendon Healing

Qi Tan,[1,2,*] Pauline Po Yee Lui,[3,*] and Yuk Wa Lee[1,2]

We investigated the spatial distribution of stem cells in tendons and the roles of stem cells in early tendon repair. The relationship between tendon-derived stem cells (TDSCs) isolated in vitro and tendon stem cells in vivo was also explored. Iododeoxyuridine (IdU) label-retaining method was used for labeling stem cells in rat patellar tendons with and without injury. Co-localization of label-retaining cells (LRCs) with different markers was done by immunofluorescent staining. TDSCs were isolated from patellar tendon mid-substance after IdU pulsing, and the expression of different markers in fresh and expanded cells was done by immunofluorescent staining. More LRCs were found at the peritenon and tendon–bone junction compared with the mid-substance. Some LRCs at the peritenon were located at the perivascular niche. The LRC number and the expression of proliferative, tendon-related, pluripotency, and pericyte-related markers in LRCs in the window wound increased. Most of the freshly isolated TDSCs expressed IdU, and some TDSCs expressed pericyte-related markers, which were lost during expansion. Both freshly isolated and subcultured TDSCs expressed pluripotency markers, which were absent in LRCs in intact tendons. In conclusion, we identified LRCs at the peritenon, mid-substance, and tendon–bone junction. There were both vascular and non-vascular sources of LRCs at the peritenon, while the source of LRCs at the mid-substance was non-vascular. LRCs participated in tendon repair via migration, proliferation, activation for tenogenesis, and increased pluripotency. Some LRCs in the window wound were pericyte like. Most of the mid-substance TDSCs were LRCs. The pluripotency markers and pericyte-related marker in LRCs might be important for function after injury.

Introduction

Adult stem cells are capable of producing daughter cells of their own for tissue homeostasis or tissue replacement after injury. It is assumed that stem cells are activated in response to injury signals. Typical examples are hair follicle stem cells and intestinal stem cells that proliferated and differentiated for tissue repair [1,2].

Recently, stem/progenitor cells have been isolated from tendon tissues of varies species, including human, horse, rabbit, rat, and mouse [3–6]. These stem/progenitor cells isolated from tendon tissues exhibited self-renewal and multilineage differentiation potential [3–6]. Since the origin and identity of these cells were not clear, we called them tendon-derived stem cells (TDSCs) to indicate only the tissue from which the cells were isolated [5].

Many studies suggested that the wall of capillaries, small vessels, and large vessels harbored stem/progenitor cells [7–11]. Some studies further suggested that mesenchymal stem cells (MSCs) were derived from pericytes [9,12]. Pericytes/perivascular cells from a variety of tissues were reported to exhibit characteristics that were strikingly similar to those of MSCs [7–11]. For tendons, there was also evidence that the vasculature of tendon tissue might harbor stem cells [13]. However, tendon mid-substance is hypovascular compared with other tissues and receives its blood supply mainly from the endotenon and paratenon [14]. TDSCs isolated from the tendon mid-substance, while positive for alpha smooth muscle actin [5], were not positive for other pericyte-related markers [3,15]. Tendon stem cells either might have lost the pericyte-related markers during in vitro subculture and/or there might be more than one source of stem cells in tendons.

As stem cells residing in tendon tissues, tendon stem cells are expected to play roles in tendon homeostasis. Whether and how they participate in tendon repair has not been studied. In this study, we took advantage of the slow-cycling or asymmetric-cell division with nonrandom-chromosomal-cosegregation (ACD-NRCC) properties of stem cells to investigate the spatial distribution of stem cells in tendons and how stem cells participate at the early stage of tendon repair

[1]Department of Orthopaedics and Traumatology, and [2]The Hong Kong Jockey Club Sports Medicine and Health Sciences Centre, Faculty of Medicine, The Chinese University of Hong Kong, Hong Kong SAR, China.
[3]Headquarter, Hospital Authority, Hong Kong SAR, China.
*These two authors have contributed equally to this work.

after injury using the iododeoxyuridine (IdU) label-retaining method [16–19]. The relationship between TDSCs isolated in vitro and tendon stem cells in vivo was also explored. We hypothesized that (1) the IdU label-retaining cells (LRCs) could be identified at the peritenon, tendon mid-substance, and tendon–bone junction; (2) some, but not all, LRCs could be identified at the perivascular niche; (3) LRCs might contribute to tendon repair by cell migration, proliferation, activation for tenogenesis, and increased pluripotency; (4) some LRCs in the window wound were pericyte like; (5) TDSCs were LRCs and there was loss of pericyte-related marker during subculture; and (6) there was activation of pluripotency markers and pericyte-related marker in TDSCs, in which the process of cell isolation mimics tendon injury.

Materials and Methods

Study design

All the animal experiments were approved by the animal research ethics committee of the authors' institution. The use of nucleotide analogs such as IdU to label stem cells in vivo has been widely reported [16,17]. Stem cells are hypothesized to preferability retain the nucleotide analogs due to their slow cycling property or by ACD-NRCC [16–19]. In this study, thirty-three 1-day-old Sprague–Dawley male rats (8–10 g) were given an intraperitoneal injection of IdU (Sigma-Aldrich, St Louis, MO) at 0.1 mg/g body weight for 5 consecutive days in order to label the stem cells in tendons. The rats were then divided into three groups for three different parts of the study. In Part I, 15 rats were killed and one patellar tendon was harvested from each rat at weeks 4, 6, and 8 after IdU pulsing (5 rats/time point). The percentages of IdU+ cells at the peritenon, mid-substance, and tendon–bone junction excluding the hypertropic chondrocyte zone were counted and the expression of Ki67, a cell proliferation marker, in IdU+ cells at different regions was compared after co-immunofluorescent staining. The co-localization of LRCs (stable IdU+ cells) with pericytes at the peritenon, mid-substance, and tendon–bone junction excluding the hypertropic chondrocyte zone was also examined by co-immunofluorescent staining with a pericyte-related marker (CD146) [20]. The co-localization of LRCs with CD44 and Sca-1, two commonly used in vitro MSC markers, in the mid-substance in intact tendon and at the window wound at day 7 after injury (see protocol below) was examined by co-immunofluorescent staining. Consecutive sections to the sections stained with CD146 and Sca-1 were stained with hematoxylin and eosin (H&E) for comparison.

In Part II, a window wound of 1 mm in diameter was created in the patellar tendon of another 15 rats (weight: 150–200 g) at week 6 after IdU pulsing as previously described [21]. The intact patellar tendon in the contralateral limb of each rat served as a control. At days 3, 7, and 14 after injury (5 rats/time point), the injured patellar tendon and the contralateral intact patellar tendon of each rat were harvested for histology for the examination of the window wound; and immunofluorescent staining of IdU and co-staining with (1) Ki67 for studying LRC proliferation; (2) scleraxis, tenomodulin, and smad8 for studying the activation of tenogenesis in LRCs; (3) Oct4, Nanog, Sox2, and nucleostemin for studying pluripotency of LRCs; and (4) CD146 for studying the pericyte-related origin of LRCs in the window wound. The percentage and the fluorescent intensity of LRCs in the window wound were compared with those in the intact patellar tendons and with time after tendon injury.

In Part III, TDSCs were isolated from the patellar tendon mid-substance of three rats (weight: 150–250 g) at weeks 6–8 after IdU pulsing (one at week 6 and two at week 8 after IdU pulsing). The expression of IdU, Oct4, Nanog, Sox2, nucleostemin, and CD146 in the freshly isolated (day 3) and expanded (day 10)/subcultured (P1) TDSCs was examined.

Animal surgery

Fifteen Sprague Dawley male rats were used in this study. The rats were anesthetized by an intramuscular injection of 10% ketamine/2% xylazine (Kethalar, 0.3 mL: 0.2 mL) and maintained sedation by 10% ketamine injected intravenously (Sigma Chemical CO, St. Louis, MO). To create the tendon defect, the central portion of the patellar tendon ($\sim$1 mm in width) was removed from the distal apex of the patella to the insertion of the tibia tuberosity without damaging the fibrocartilage zone with three stacked sharp blades as described in the previous study [21]. The wound was then closed in layers. The animals were allowed to have free-cage activity until euthanasia.

Histology and immunofluorescent staining

The patellar tendon was frozen, embedded in Tissue-TekOTC compound (Sakura Finetek, Torrance, CA), and stored at -80°C until use. The blocks were cut in the coronal plane along the length of the patella tendon to 5-μm-thick sections.

For the histological analysis, the frozen sections were stained with H&E and examined under light microscopy (DMRXA2; Leica Microsystems Wetzlar GmbH, Wetzlar, Germany).

For the immunofluorescent analysis, the frozen sections were fixed in 4% paraformaldehyde in phosphate buffered saline (PBS) (pH 7.4) for 15 min at room temperature. Antigen retrieval and cell permeabilization were done by heating the sections in citrate butter (pH 6) for 30 min. Afterward, nonspecific binding was blocked with 10% serum from the species that the secondary antibody was raised in PBS with 1% bovine serum albumin (blocking buffer) for 1 h at room temperature (Table 1). Primary antibodies in the same blocking buffer were applied to the sections overnight at 4°C. After washing, Alexa Fluor-conjugated secondary antibodies in blocking buffer were added to the sections for 1 h at room temperature in the dark (Table 1). The study of co-localization of a second target marker was done as necessary with similar immunofluorescent staining protocol. The sections were then counterstained with the nuclear stain 4′,6-diamidino-2-phenylindole in ProLong® Gold Antifade Reagent (Life Technology, Carlsbad, CA). The sections were then mounted on cover slips and examined with a fluorescent microscope equipped with a UV laser (ZEISS AxioPlan 2; Carl Zeiss MicroImaging LLC, Jena, Germany) at different emission and excitation wavelengths (Table 1). The IdU+ signal alone, its co-localization with different markers, and light microscopic images of unstained sections were captured and overlaid by the SPOT image software (SPOT Imaging Solutions, MI).

Table 1. Conditions for Immunofluorescent Staining

Marker	*Blocking*	*Primary antibody (company, dilution)*	*Secondary antibody (company, dilution)*	*Emission and excitation wavelengths*
IdU	10% Goat serum in PBS with 1% BSA for 1 h	Mouse anti-IdU (Abcam, Cambridge, UK; 1:100)	Alexa Fluor 488 goat anti-mouse (Life Technologies, Carlsbad, CA; 1:500)	Excitation: 450–490 nm; Emission: 515–565 nm
Ki67	10% Goat serum in PBS with 1% BSA for 1 h	Rabbit anti-Ki67 (Abcam; 1:100)	Alexa Fluor 594 goat anti-rabbit (Life Technologies; 1:500)	Excitation: 546/12 nm; Emission: 590 nm
CD146	10% Goat serum in PBS with 1% BSA for 1 h	Rabbit anti-CD146 (Abcam; 1:100)	Alexa Fluor 594 goat anti-rabbit (Life Technologies; 1:500)	Excitation: 546/12 nm; Emission: 590 nm
CD44	10% Goat serum in PBS with 1% BSA for 1 h	Rabbit anti-CD44 (Abcam; 1:100)	Alexa Fluor 594 donkey anti goat (Life Technologies; 1:500)	Excitation: 546/12 nm; Emission: 590 nm
Sca-1	10% Goat serum in PBS with 1% BSA for 1 h	Rabbit anti Sca-1 (Merck Millipore, Billerica, MA; 1:200)	Alexa Fluor 594 goat anti-rabbit (Life Technologies; 1:500)	Excitation: 546/12 nm; Emission: 590 nm
Scleraxis (Scx)	10% Goat serum in PBS with 1% BSA for 1 h	Rabbit anti-scleraxis (Abcam; 1:100)	Alexa Fluor 594 goat anti-rabbit (Life Technologies; 1:500)	Excitation: 546/12 nm; Emission: 590 nm
Tenomodulin (Tnmd)	10% Donkey serum in PBS with 1% BSA for 1 h	Goat anti-Tnmd (Santa Cruz, Dallas, TX; 1:100)	Alexa Fluor 594 donkey anti-goat (Life Technologies; 1:500)	Excitation: 546/12 nm; Emission: 590 nm
Smad8	10% Goat serum in PBS with 1% BSA for 1 h	Rabbit anti-smad8 (Cell Signaling, Danvers, MA; 1:100)	Alexa Fluor 594 goat anti-rabbit (Life Technologies; 1:500)	Excitation: 546/12 nm; Emission: 590 nm
Oct4	10% Goat serum in PBS with 1% BSA for 1 h	Rabbit anti-Oct4 (Abcam; 1:100)	Alexa Fluor 594 goat anti-rabbit (Life Technologies; 1:500)	Excitation: 546/12 nm; Emission: 590 nm
Nanog	10% goat serum in PBS with 1% BSA for 1 h	Rabbit anti-Nanog (Abcam; 1:100)	Alexa Fluor 594 goat anti-rabbit (Life Technologies; 1:500)	Excitation: 546/12 nm; Emission: 590 nm
Sox2	10% Goat serum in PBS with 1% BSA for 1 h	Rabbit anti-Sox2 (Abcam; 1:100)	Alexa Fluor 594 goat anti-rabbit (Life Technologies; 1:500)	Excitation: 546/12 nm; Emission: 590 nm
Nucleostemin	10% Goat serum in PBS with 1% BSA for 1 h	Rabbit anti-nucleostemin (Abcam; 1:100)	Alexa Fluor 594 goat anti-rabbit (Life Technologies; 1:500)	Excitation: 546/12 nm; Emission: 590 nm

IdU, iododeoxyuridine; PBS, phosphate buffered saline; BSA, bovine serum albumin.

Image analysis

One section from each sample was used in image analysis. Fluorescent images were acquired under the same exposure settings for all sections in each experiment of the study. To count the number of IdU+ cells at the peritenon, mid-substance, and tendon–bone junction excluding the hypertropic chondrocyte zone or window wound after injury, three views of 0.29 mm × 0.22 mm were randomly selected in each tendon region of one section of each tendon sample. The number of IdU+ cells in each view was counted using the Adobe Photoshop software (version 7.0; San Jose, CA), and the percentage of IdU+ cells was reported. Fluorescent intensity of IdU+ cells was measured using the ImageJ software (NIH Image, National Institutes of Health, Bethesda, MD; online at: http://rsbweb.nih.gov/ij/). First, the color image in red, green, blue format was converted to grayscale image. The target cell was then selected by drawing a rectangle around the cell. Select "Area," "Integrated Density," and "Mean Gray Value" in "Set Measurements" from the Analyze menu. Select "Measure" function from the Analyze menu. To correct for the background noise, four regions next to the target cell were selected and the area, integrated density, and mean gray value of each of these regions were measured in a similar fashion. The mean of mean gray value of these background regions was calculated. The corrected total cell fluorescence (CTCF) of the target cell was calculated using the following formula:

$$\text{CTCF} = \text{Integrated density} - (\text{area of target cell} \times \text{mean of mean gray value of background regions})$$

The fluorescent intensity of at least 20 IdU+ cells in the mid-substance in the control group and at least 50 IdU+ cells in the window wound in the injury group at different times after injury was measured, averaged, and normalized with the fluorescent intensity of the control group at day 3. To calculate the percentage of LRCs in the window wound that was Ki67 positive, an area of 0.58 mm × 0.43 mm was randomly selected in the window wound and the number of IdU+ cells and IdU+Ki67+ cells were counted. Representative images matching the conclusion of the experiment were shown. The peritenon was defined as the loose

connective tissue surrounding the tightly packed tendon mid-substance from the distal apex of the patella to the insertion of the tibia tuberosity without inclusion of the fibrochondrocytes (Supplementary Fig. S1; Supplementary Data are available online at www.liebertpub.com/scd). Fibrochondrocytes at the tendon–bone junction that were round but not yet displaying the typical hypertropic chondrocyte phenotype were examined (Supplementary Fig. S1). The cells in this region could be easily recognized in the fluorescence image as the high concentration of cells between the longitudinally aligned cells at the tendon mid-substance and the large randomly oriented cells at the junction (Supplementary Fig. S1).

TDSC isolation and culture

Three 7–9-week-old IdU-labeled male Sprague–Dawley rats (one at week 6 and two at week 8 after IdU pulsing), weighing 150–220 g, were used for TDSC isolation as previously described [22]. Briefly, the rats were euthanized with an overdose (about 1 mL) of 20% sodium phenobarbital intraperitoneal. The mid-substances of both patellar tendons were excised. Care was taken that only the mid-substance of patellar tendon tissue, but not the tissue at the tendon–bone junction, was collected. The peritenon was carefully removed, and the tissue was stored in sterile PBS. The tissue was minced, digested with type I collagenase (3 mg/mL; Sigma-Aldrich), and passed through a 70 μm cell strainer (Becton Dickinson, Franklin Lakes, NJ) to yield a single-cell suspension. The released cells were washed in PBS and resuspended in low-glucose Dulbecco's modified Eagle medium (Gibco BRL; Life Technologies, Invitrogen, Carlsbad, CA), 10% fetal bovine serum, 50 μg/mL penicillin, 50 μg/mL streptomycin, and 100 μg/mL neomycin (complete culture medium) (all from Invitrogen Corporation, Carlsbad, CA). The isolated nucleated cells were plated at an optimal low density (500 cells/cm^2) for the isolation of TDSCs from rat patellar tendon and cultured at 37°C, 5% CO_2 to form colonies. At day 3 after initial plating, the cells were washed twice with PBS to remove the non-adherent cells and were called freshly isolated TDSCs. At days 7–10, they were trypsinized and mixed together as passage 0 (P0). TDSCs were subcultured at 4,000 cells/cm^2 when they reached 80%–90% confluence. Medium was changed every 3 days. Freshly isolated TDSCs at day 3, day 10, or TDSCs at P1 were used for immunofluorescent staining as described earlier after in-situ fixation in 4% paraformaldehyde in PBS (pH 7.4) for 15 min at room temperature.

Data analysis

Quantitative data were presented as mean ± SD and shown in boxplots. A comparison of two independent groups was done using Mann–Whitney *U* test, while a comparison of more than two independent groups was done by Kruskal–Wallis test followed by post-hoc comparison using Mann–Whitney *U* test. All the data analysis was done using SPSS software (SPSS, Inc., Chicago, IL; version 20.0). $p \le 0.050$ was regarded statistically significant.

Results

Time-dependent changes of IdU+ cells

To determine the optimal time for studying LRCs in tendons after pulsing with IdU label, we studied the percentage of IdU+ cells in the tendon mid-substance at weeks 4, 6, and 8 after pulsing. Our results showed that IdU+ cells were evenly distributed within the parallel collagen fibers (Fig. 1A–C, white arrows). No IdU+ cell cluster was observed. There was significantly higher IdU+ cells in the tendon mid-substance at week 4 compared with that at week 6 (10.9% ± 5.2% vs. 3.2% ± 0.8%; overall $p < 0.005$; post-hoc $p < 0.01$) and at week 8 (10.9% ± 5.2% vs. 2.3% ± 0.6%; post-hoc $p < 0.01$) (Fig. 1D). While some IdU+ cells were proliferating at week 4 (Fig. 1A, yellow arrows), none of them were proliferating at weeks 6 and 8 (Fig. 1B, C). Since the number of IdU+ cells became stable from weeks 6 to 8 (post-hoc $p = 0.076$) (Fig. 1D), the subsequent studies were done using rats that have been labeled for 6–8 weeks.

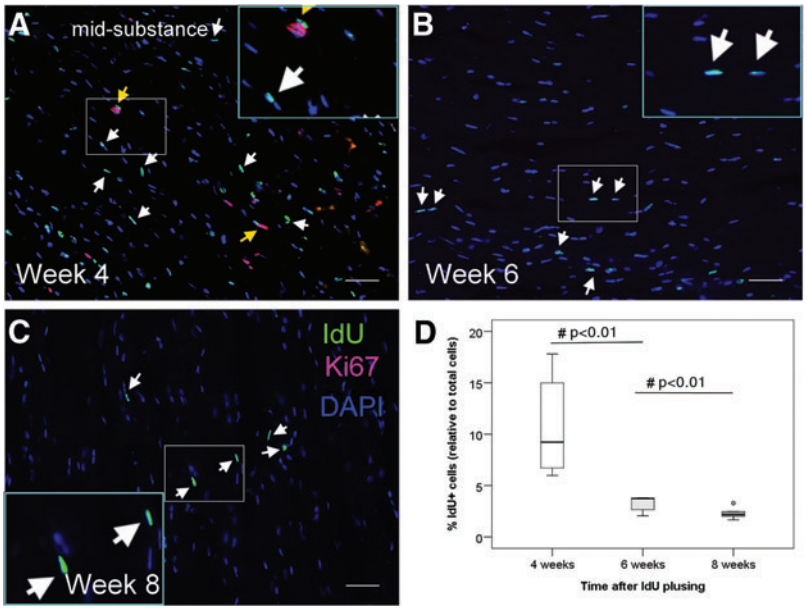

FIG. 1. Time-dependent changes of iododeoxyuridine (IdU)+ cells. Photomicrographs showing the IdU+ cells and their co-localization with Ki67 at the tendon mid-substance at **(A)** weeks 4, **(B)** 6, and **(C)** 8 after IdU pulsing. The *blue box* is the magnified view of the *white box*. Scale bar = 50 μm (*outer image*); *white arrows*: IdU+ cells; *yellow arrows*: IdU+ Ki67+ cells; **(D)** Boxplot showing the percentage of IdU+ cells at the mid-substance at weeks 4, 6, and 8 after IdU pulsing. "o" represents outliner of the dataset. #post-hoc $p \le 0.050$. Color images available online at www.liebertpub.com/scd

Spatial distribution of LRCs in tendon

LRCs could be observed at the peritenon, mid-substance, and tendon–bone junction (Fig. 2A). LRCs at the tendon–bone junction were clustered at the zone with small and round cells; and they could not be detected at the zone with hypertropic chondrocyte-like cells (Fig. 2A). More LRCs were observed at the peritenon (7.4%±1.8%; overall $p<0.01$; post-hoc $p=0.02$) and tendon–bone junction excluding the hypertropic chondrocyte zone (9.4%±3.2%; post-hoc $p<0.02$) compared with that at the mid-substance (3.9%±1.3%) (Fig. 2B). Some LRCs at the peritenon, but not LRCs at the tendon mid-substance, were proliferating as shown by the Ki67 signal (Fig. 2A, yellow arrows). CD146 was expressed only at the peritenon (Fig. 2C). Some, but not all CD146 signals, were seen on the vascular features at the peritenon, and all vascular features were intensively stained with CD146 (Fig. 2C). No vascular features could be found at the tendon mid-substance. Some LRCs were located close to the perivascular niche at the peritenon (Fig. 2C). Some LRCs co-localized with CD146 at the peritenon (Fig. 2C, yellow arrows).

Co-localization of LRCs with CD44 and Sca-1

Most of the cells, including LRCs, at the mid-substance of intact patellar tendon and in the window wound at week 1 were stained with CD44 and Sca-1 (Fig. 3). The signal intensity of CD44+ and Sca+ cells increased in the window wound at day 7 after injury.

Presence and proliferation of LRCs in response to tendon injury

LRCs were observed in the window defect at day 3 after injury, increased at day 7 (overall $p<0.005$, post-hoc $p<0.01$), and reduced at day 14 (vs. day 3: post-hoc $p<0.01$; vs. day 7: post-hoc $p<0.01$) (Fig. 4D–F, G, white arrows). Compared with a similar tendon region in the intact control group (Fig. 4A–C), there were significantly more LRCs in the window wound at day 3 ($p<0.05$; 7.1%±1.9% vs. 4.2%±1.5%) and day 7 ($p<0.01$; 29.6%±6.3% vs. 3.4%±0.9%) but less LRCs at day 14 ($p<0.01$; 0.07%±0.08% vs. 2.5%±0.3%) after injury (Fig. 4G). The normalized fluorescent intensity of LRCs in the window wound in the injured tendon at day 7 ($p<0.01$) and day 14 ($p<0.01$) was also weaker than that in the intact tendon control (Fig. 4H). While all LRCs in the intact tendon mid-substance did not express Ki-67 (Fig. 4A–C), 6.5%+0.9% and 8.4%+0.7% of all the LRCs in the window wound were Ki67+ at days 3 and 7, respectively (Fig. 4D, E, yellow arrows). There was nearly no LRCs and, hence, Ki67+ LRCs in the window defect at day 14 (Fig. 4F).

Expression of tendon-related markers in LRCs in response to tendon injury

To investigate the activation of tenogenesis of LRCs in response to tendon injury, we co-localized the tendon-related markers, including scleraxis, tenomodulin, or smad8 with LRCs. At days 3, 7, and 14 after injury, the expression of

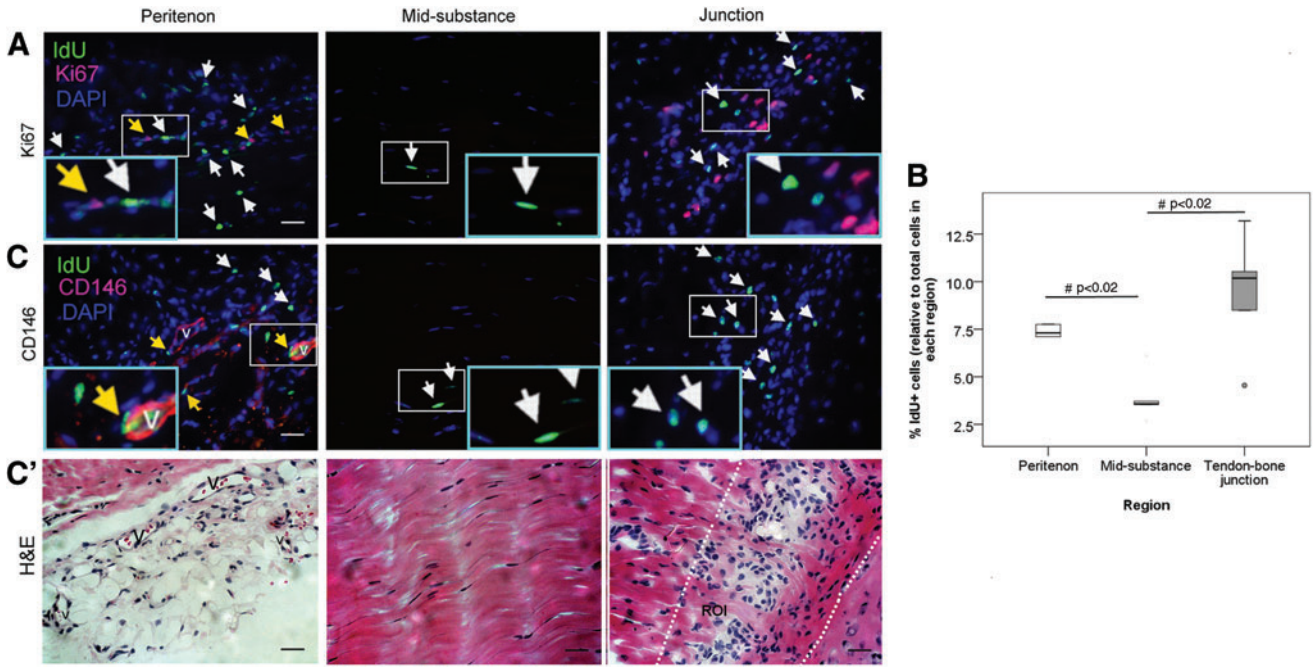

FIG. 2. Spatial distribution of label-retaining cells (LRCs) in tendon. **(A, C)** Photomicrographs showing the IdU+ cells and their co-localization with **(A)** Ki67 and **(C)** CD146 at the peritenon, mid-substance, and tendon–bone junction at week 6 after IdU pulsing. The *blue box* is the magnified view of the *white box*. Scale bar = 25 μm (*outer image*); V (label placed inside lumen): vascular feature; *white arrows*: IdU+ cells; *yellow arrows*: IdU+ cells co-localized with target marker; *Panel* **(C')** shows the hematoxylin and eosin (H&E) staining of the adjacent consecutive sections of *panel* **(C)**. Scale bar = 25 μm; V (label placed inside lumen): vascular feature; The two *dotted lines* in the last H&E photo indicated the region of interest (ROI) for cell counting at the tendon–bone junction excluding the hypertrophic chondrocyte zone. **(B)** Boxplot showing the percentage of IdU+ cells at the peritenon, mid-substance, and tendon–bone junction at week 6 after IdU pulsing. "o" represents outliner of the dataset. #post-hoc $p \le 0.050$. Color images available online at www.liebertpub.com/scd

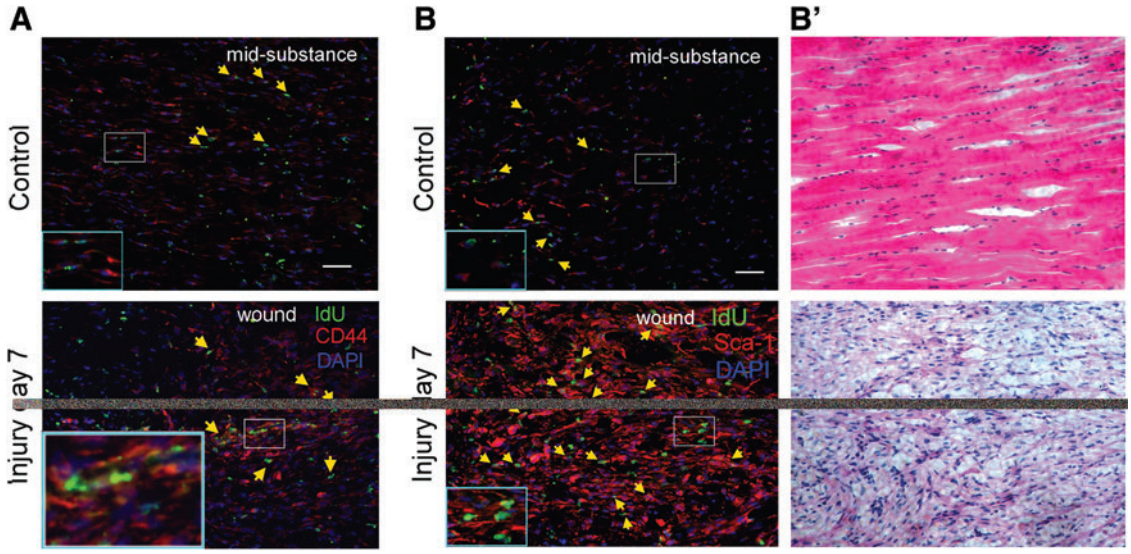

FIG. 3. Co-localization of CD44 and Sca-1 with LRCs in tendon. Photomicrographs showing the IdU+ cells and their co-localization with **(A)** CD44 and **(B)** Sca-1 in the mid-substance in the intact tendon and at the window wound at day 7 after tendon injury. *Panel* **(B′)** shows the H&E staining of the adjacent consecutive sections of *panel* **(B)**. The *blue box* is the magnified view of the *white box*. Scale bar = 50 μm (outer image); *yellow arrows*: IdU+ cells co-localized with target marker. Color images available online at www.liebertpub.com/scd

scleraxis, tenomodulin, and smad8 increased dramatically in the window wound compared with the mid-substance of the uninjured contralateral control group (Fig. 5). Most of the LRCs in the window wound also showed increased expression of scleraxis, tenomodulin, and smad8 (Fig. 5, yellow arrows).

Expression of pluripotency markers in LRCs in response to tendon injury

To investigate the pluripotency of LRCs, the pluripotency markers, including Oct4, Nanog, Sox2, and nucleostemin, were co-localized with LRCs in injured and contralateral uninjured tendons. No LRCs in the contralateral intact tendon mid-substance expressed Oct4, Nanog, Sox2, and nucleostemin (Fig. 6). However, at days 3, 7, and 14 after injury, many cells in the window wound expressed Oct4, Nanog, Sox2, and nucleostemin. The majority of LRCs in the window wound were positive for Oct4, Nanog, Sox2, and nucleostemin (Fig. 6, yellow arrows).

Expression of pericyte-related markers in LRCs in response to tendon injury

We also studied the relationship between pericytes and LRCs during tendon healing. There was expression of CD146 in the healing tendon cells (*) and the vascular features (V) in the window wound at days 3, 7, and 14 after tendon injury, which was not observed in the mid-substance of intact tendon (Fig. 7). Some LRCs in the window wound were positive for CD146 (Fig. 7, yellow arrows). Some LRCs in the window wound were located close to the vascular features, which were not observed in the intact tendon mid-substance (Fig. 7).

Characterization of LRCs and TDSCs in vitro

Most (about 75%) of the freshly isolated TDSCs at day 3 expressed IdU (Fig. 8A) and some (about 25%) TDSCs expressed CD146 (Fig. 8C). However, the expression of IdU and CD146 was lost during in vitro expansion at day 10 (Fig. 8B) and P1 (Fig. 8D), respectively. Both freshly isolated and subcultured P1 TDSCs expressed pluripotency markers, including Oct4 (Fig. 8E, F), Nanog (Fig. 8G, H), Sox2 (Fig. 8I, J), and nucleostemin (Fig. 8K, L), which were absent in the mid-substance in intact tendons (Fig. 6). The expression of these markers was stronger in the center of TDSC colonies.

Discussion

Despite the identification and isolation of stem cells from tendon tissues, the in vivo identity and the roles of these cells in tendon homeostasis remained unclear. Using the IdU label-retaining method, this study was set forth to understand the in vivo location of stem cells in tendons and the roles of stem cells during tendon repair. A better understanding of these characteristics of stem cells in tendons might provide insights for understanding the slow and poor healing quality of tendon; and for the development of therapeutic strategies for mobilizing these cells for tendon repair.

Spatial localization of LRCs

Our results showed that LRCs could be identified at the peritenon, tendon mid-substance, and tendon–bone junction. 3%–4% of LRCs were present in the tendon mid-substance, similar to the percentages of stem cells derived from tendon mid-substance in vitro [3,5]. Most of the freshly isolated TDSCs using our standard protocol for stem cell isolation from tendon expressed IdU, suggesting that LRCs were likely to be TDSCs isolated from tendon tissues. This was the first report of resident stem cells at the tendon–bone junction, which might be important for its repair and maintenance. More LRCs could be found at the peritenon and tendon–bone junction excluding the hypertropic chondrocyte zone compared with those at the tendon mid-substance. The

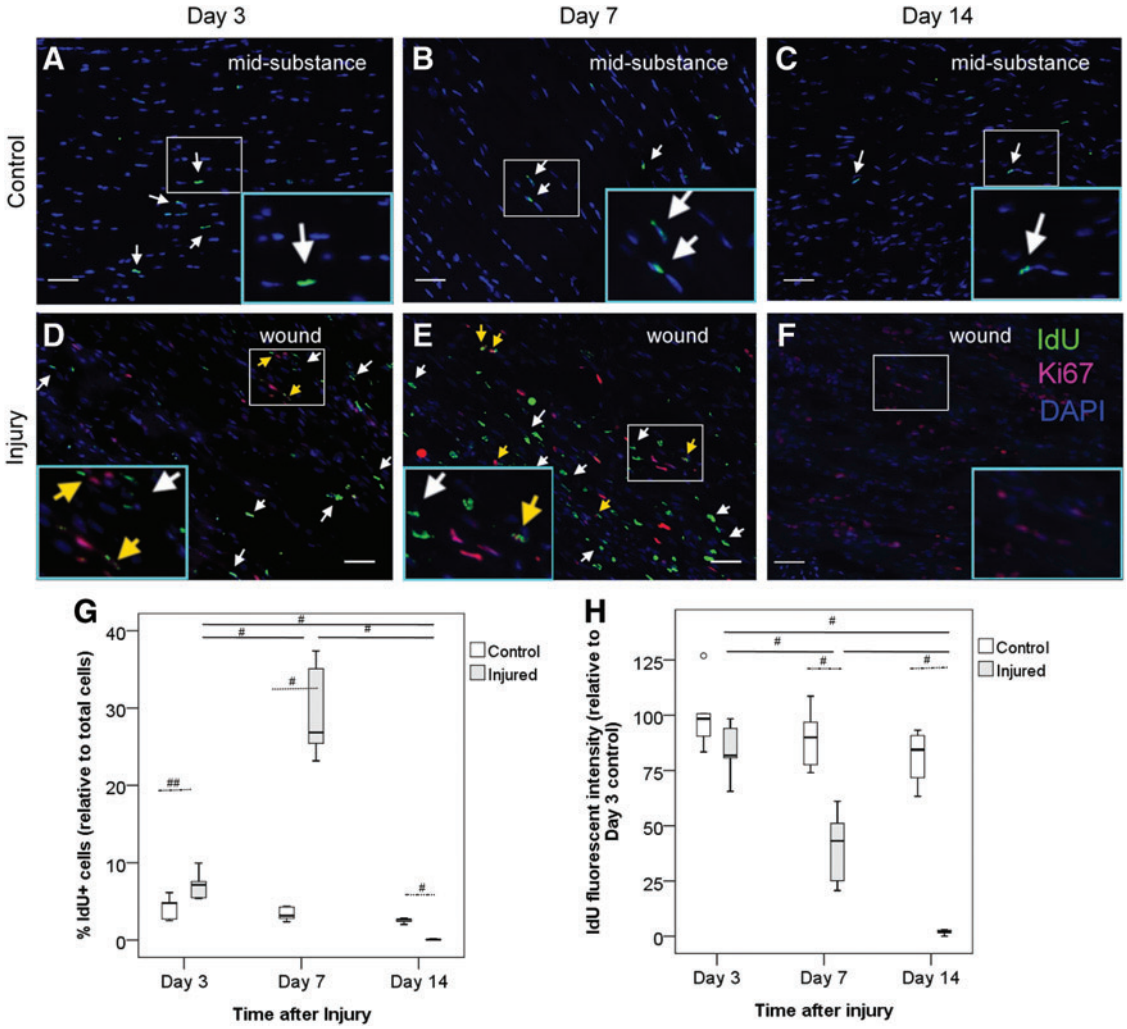

FIG. 4. Presence and proliferation of LRCs in response to tendon injury. Photomicrographs showing the IdU+ cells and their co-localization with Ki67 at the window wound at **(D)** days 3, **(E)** 7, and **(F)** 14 after tendon injury. **(A–C)** Intact tendon mid-substance harvested at the same time points served as controls. The *blue box* is the magnified view of the *white box*. Scale bar = 50 μm (outer image); *white arrows*: IdU+ cells; *yellow arrows*: IdU+ Ki67+ cells; **(G, H)** Boxplots showing the percentage of IdU+ cells **(G)** and the averaged fluorescent intensity of IdU+ cells at the window wound at days 3, 7, and 14 after tendon injury normalized with the averaged fluorescent intensity of IdU+ cells at day 3 in the control group **(H)**. "o" represents outliner of the dataset. $^{\#}p < 0.02$; $^{\#\#}p < 0.05$. Color images available online at www.liebertpub.com/scd

origins of LRCs were likely to be different at the peritenon and tendon mid-substance. While all the LRCs were seen embedded between parallel collagen fibers at the tendon mid-substance, some LRCs were found at the perivascular niche at the peritenon. Mienaltowski et al. [23] also reported the existence of different stem/progenitor cell populations within distinct niches at the tendon mid-substance and peritenon; and the stem/progenitor cells at the peritenon might be more vascular in origin. Bi et al. [3] reported the residence and alignment of LRCs in-between long parallel collagen fibrils containing biglycan and fibromodulin [3]. The significance of localization of IdU+ cells at the peritenon and the mid-substance was not clear but might be important for extrinsic and intrinsic repair of tendon, respectively [23].

Role of LRCs during tendon repair

Using co-immunofluorescent staining, we showed that LRCs migrated, proliferated, activated for tenogenesis, and showed increased pluripotency at the window wound after tendon injury. The decrease in the number of LRCs at day 14 after tendon injury was likely to be due to the rapid depletion of IdU label as a result of rapid cell proliferation as we observed punctuated staining of the IdU label in cells expressing Ki67. This also explained the high number but low fluorescent intensity of IdU+ cells in the window wound at day 7. The participation of endogeneous stem cells in tissue repair via migration, proliferation, and differentiation was also reported in other tissues. Using the bromodeoxyuridine label-retaining method, Kurth et al. reported that MSCs identified in vivo in the knee joint synovium proliferated and differentiated into chondrocytes in areas of cartilage metaplasia within the synovium after articular cartilage injury [16]. Using a genetic lineage tracing technique, Feng et al. [24] has recently demonstrated the direct differentiation of a small percentage of genetically marked pericytes to odontoblasts both during incisor growth and repair after damage. A population of MSC-like cells was observed to directly

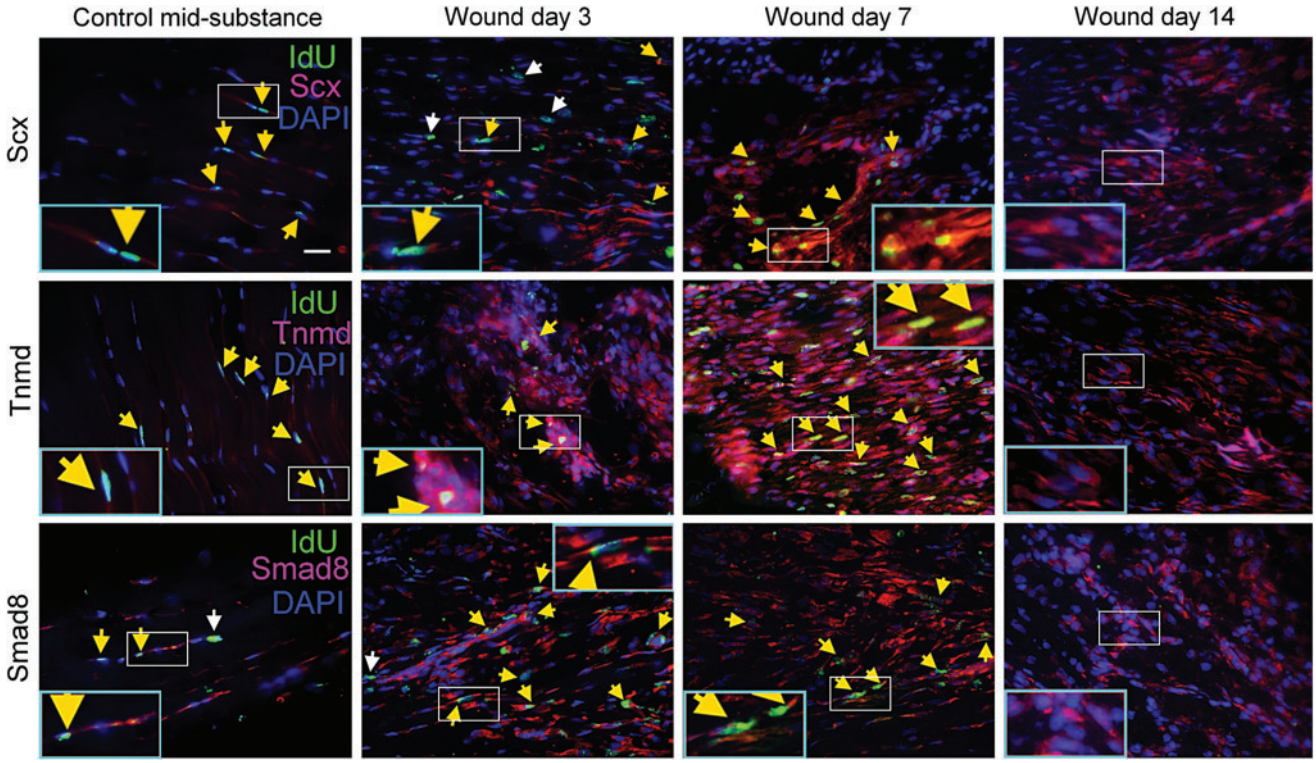

FIG. 5. Activation of tenogenesis of LRCs in response to tendon injury. Photomicrographs showing the IdU+ cells and their co-localization with scleraxis, tenomodulin, or smad8 at the window wound at days 3, 7, and 14 after tendon injury. Contralateral intact tendon mid-substance harvested at day 3 after injury served as controls. The *blue box* is the magnified view of the *white box*. Scale bar = 25 μm (outer image); *white arrows*: IdU+ cells; *yellow arrows*: IdU+ cells co-localized with target marker. Color images available online at www.liebertpub.com/scd

migrate from the cervical end of incisor toward the damaged area, differentiate, and contribute to the majority of odontoblasts during repair [24].

It should be noted that there was lower expression of the tendon-related markers in the LRCs and even in the tenocytes in the mid-substance in the intact tendon compared with the cells in the window wound, suggesting that these tendon-related markers were important for tendon repair and their expression was likely to reduce at the end of tendon repair.

The sources of LRCs contributing to tendon repair was not clear from this study, as all the potential stem cells in the body were labeled. We observed increased expression of CD146 in the window wound, which was absent in the intact tendon. Some LRCs in the window wound expressed CD146, suggesting that they were pericyte like. Some LRCs in the window wound were located close to the vascular structures, which were not observed in the intact tendon mid-substance. This suggested that there was likely a vascular source, in addition to a non-vascular source, of LRCs for tendon repair.

We also observed that the majority of LRCs in the window defect expressed pluripotency markers, and this was not observed in the mid-substance of intact patellar tendon. Our result was consistent with the hypothesis that the developmental program might be re-activated during tendon repair, as a previous study showed that there were similar gene expression patterns and structural changes in healing and developing tendons [25]. However, natural adult tendon healing is characterized by scar tissue formation, ectopic bone formation [26], and poor mechanical properties of repaired tissue long time after injury [27]. We speculated that this might be due to insufficient activation of developmental and tenogenic programs as well as erroneous differentiation of stem cells. Further research is required to confirm this. The lack of expression of these pluripotency markers in intact patellar tendon suggested that immunohistochemical staining of these markers was not suitable for the detection of tendon stem cell in intact tendon in situ. The activation of Oct4, Nanog, Sox2, and nucleostemin as well as CD146 after tendon injury might be related to the functions of these proteins in regulating self-renewal, cell proliferation, differentiation, and/or angiogenesis [28–32].

Previous studies have demonstrated the expression of scleraxis [33–35], Nanog [36], and Sox 2 [37] in the cytoplasm. Although these transcription factors function in the cell nucleus, stimulatory signal is likely required to induce their translocation to the cell nucleus.

Most TDSCs are LRCs and activation of LRCs after isolation

Our results showed that there was loss of IdU label and CD146 during in vitro expansion of TDSCs. TDSCs expressed Nanog, Oct4, Sox2, and nucleostemin that were not observed in LRCs in intact tendon in vivo. The isolation of LRCs induced trauma to tendon, and this might trigger processes similar to tendon injury [28]. The expression of pluripotency markers and pericyte-related markers after

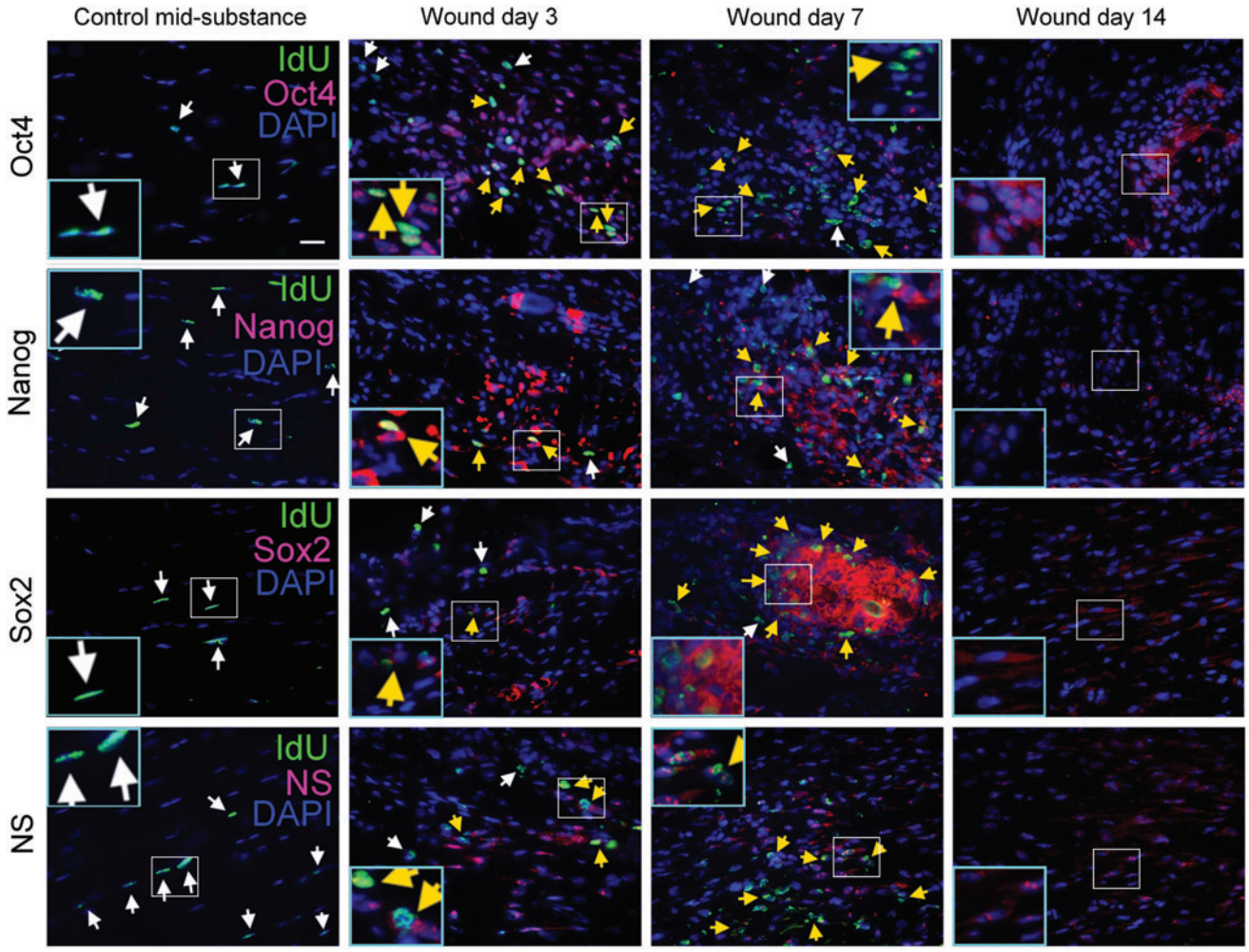

FIG. 6. Expression of pluripotency markers in LRCs in response to tendon injury. Photomicrographs showing the IdU+ cells and their co-localization with Oct4, Nanog, Sox2, or nucleostemin at the window wound at days 3, 7, and 14 after tendon injury. Contralateral intact tendon mid-substance harvested at day 3 served as controls. The *blue box* is the magnified view of the *white box*. Scale bar = 25 μm (outer image); *white arrows*: IdU+ cells; *yellow arrows*: IdU+ cells co-localized with target marker. Color images available online at www.liebertpub.com/scd

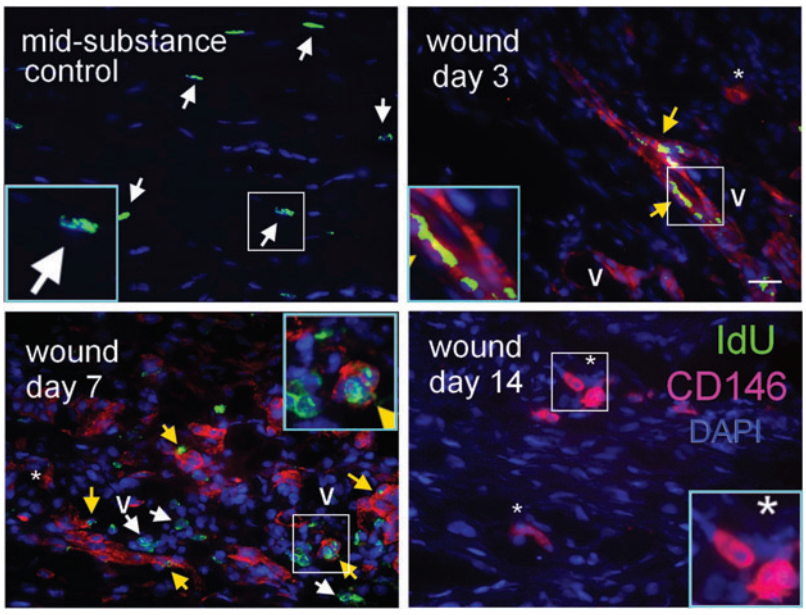

FIG. 7. Expression of pericyte-related marker in LRCs in response to tendon injury. Photomicrographs showing the IdU+ cells and their co-localization with CD146 at the window wound at days 3, 7, and 14 after tendon injury. Contralateral intact tendon mid-substance collected at day 3 after injury served as control. The *blue box* is the magnified view of the *white box*. Scale bar = 25 μm (outer image); V (label placed inside lumen): vascular feature; *: healing tendon cells; *white arrows*: IdU+ cells; *yellow arrows*: IdU+ CD146+ cells. Color images available online at www.liebertpub.com/scd

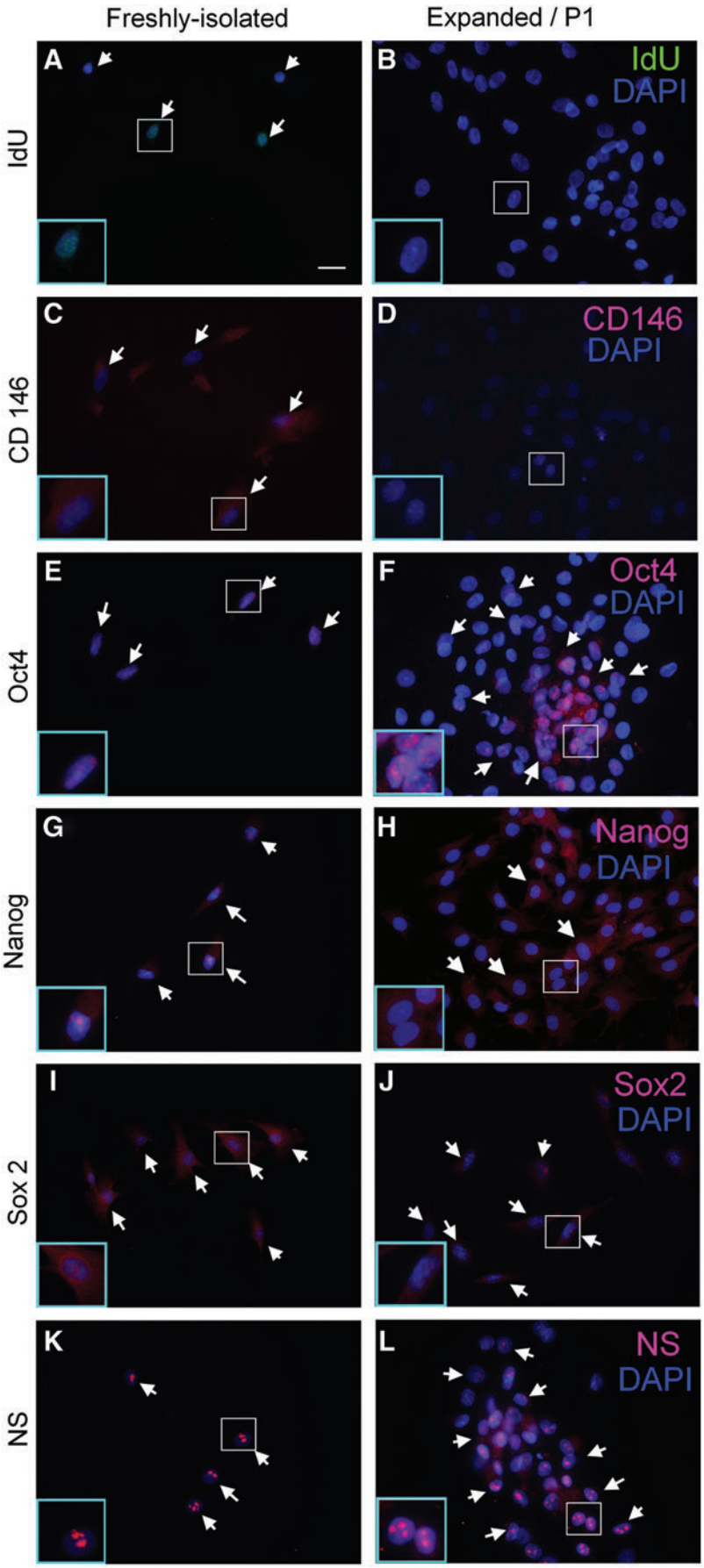

FIG. 8. Characterization of LRCs and tendon-derived stem cells (TDSCs) in vitro. Photomicrographs showing the expression of **(A, B)** IdU; **(C, D)** CD146; **(E, F)** Oct4, **(G, H)** Nanog, **(I, J)** Sox2, and **(K, L)** nucleostemin (NS) in freshly isolated TDSCs **(A, C, E, G, I)** and expanded/P1 TDSCs **(B, D, F, H, J)**. The *blue box* is the magnified view of the *white box*. Scale bar = 25 μm (outer image); *white arrows*: positive cells; blue: DAPI; *green*: IdU; *red*; CD146, Oct4, Nanog, Sox2, or nucleostemin. Color images available online at www.liebertpub.com/scd

injury in vivo and expansion in vitro suggested that these markers were important for stem cell function after injury. Moreover, the direct comparison of stem cell findings in vitro and in vivo should be cautious, as the isolated stem cells might represent the state after injury.

Limitations of this study

There is no specific marker for labeling stem cells in vivo. The position article by the International Society for Cellular Therapy on the minimal criteria for defining multi-potent mesenchymal stromal cells refers to the phenotype of stem cells isolated in vitro, not in vivo [38]. While CD73, CD90, and CD44 are commonly used for labeling MSCs in vitro, they are, in fact, not good in vivo markers. We stained CD44 and Sca-1 in the intact patellar tendon and the patellar tendon at week 1 after injury. Most of the cells, including the IdU+ cells, in the intact patellar tendon mid-substance and in the window wound were stained with CD44 and Sca-1. The signal intensity of CD44+ and Sca+ cells increased in the window wound at week 1 after injury. This makes it impossible to use these markers to label stem cells in vivo. This is also supported by previous studies which showed that lung fibroblasts also expressed CD44, CD73, and CD105 [39–41]. Other articles showed that the expression of these markers were defined operationally only aiming at enriching cells that were clonogenic/multi-potent in vitro, and none of them appeared to participate directly in the molecular processes regulating self-renewal versus differentiation [42,43]. Embryonic stem cell markers such as Oct4, Klf4, and Nanog are more specific [40], and, hence, we used some of these markers in this study for the labeling of stem cells in vitro and in vivo. On the other hand, there was no expression of Oct4, Nanog, Sox2, and nucleostemin in the intact patellar tendon as shown in this study. It is because of these reasons that we used the IdU label-retaining method for tracing the fate of endogenous slow-cycling cells which were likely to be stem cells. The IdU label-retaining method is widely used. Based on our data, the IdU+ cells observed in the present study were highly likely to be stem cells, as evident by the stable IdU+ population starting from week 6 after IdU pulsing, an important property of quiescent stem cells to retain the IdU label. Moreover, as discussed, most of the freshly isolated TDSCs based on our standard procedures for stem cell isolation from tendons expressed the IdU label. TDSCs were shown to exhibit stem cell properties, including clonogenicity and multi-lineage differentiation in many of our publications [22,44].

However, the label-retaining method has limitations. While this method is good for the study of the distribution and functions of stem cells in different tissues, it is not specific for stem cells and might label cells that have stopped proliferating due to various reasons (eg, differentiation) and, hence, might be subjected to false-positive errors. Since all the stem cells in the body were labeled, it was not clear whether the LRCs in the window wound were of the same origins as the LRCs in the intact tendons, and, hence, the LRCs in the intact tendons might not be an appropriate control. Moreover, since the IdU label was lost during cell proliferation, it could only be used to trace the early events after tissue injury. The use of other tendon stem cell tracking methods should be considered if investigators are interested in the mid-to-late events after injury [45]. The patellar tendon window injury model used in the present study is not representative of tendon ruptures observed clinically that are commonly presented with degenerative changes. The patellar tendon window injury model more closely represents the tendon-healing process at the donor site after tendon graft harvesting in anterior cruciate ligament reconstruction. The pluripotency of LRCs and TDSCs were studied by marker expression only. The expression of these markers in LRCs and TDSCs might have other functions. Further studies are required to confirm the pluripotency of these cells using functional assays.

Conclusions

In conclusion, we identified LRCs at the peritenon, tendon mid-substance, and tendon–bone junction. There were both vascular and non-vascular sources of LRCs at the peritenon, while the source of LRCs at the mid-substance was non-vascular. The LRCs participated in tendon repair after injury via migration, proliferation, activation for tenogenesis, and increased pluripotency in the window wound. Some LRCs in the window wound were pericyte like. Most of the TDSCs isolated from the tendon mid-substance were LRCs. The pluripotency markers and a pericyte-related marker in LRCs were activated after injury in vivo and isolation in vitro, suggesting that they might be important for stem cell function after injury.

Acknowledgments

This research project was supported by equipment/resources donated by the Hong Kong Jockey Club Charities Trust.

Prior conference presentation of part of the submitted material: Tan Q, Lee YW, Wong YM, and Lui PPY. In vivo identity of tendon stem cells and the roles of stem cells in tendon healing. *In Proceedings of* The 58th Annual Meeting of the Orthopaedic Research Society, 26th–29th January, 2013, Henry B. Gonzalez Convention Center, San Antonio, Texas, Oral presentation.

Author Disclosure Statement

No competing financial interests exist.

References

1. Li J, H Zheng, J Wang, F Yu, RJ Morris, TC Wang, S Huang and W Ai. (2012). Expression of Kruppel-like factor KLF4 in mouse hair follicle stem cells contributes to cutaneous wound healing. PLoS One 7:e39663.
2. Neal MD, WM Richardson, CP Sodhi, A Russo and DJ Hackam. (2011). Intestinal stem cells and their roles during mucosal injury and repair. J Surg Res 167:1–8.
3. Bi Y, D Ehirchiou, TM Kilts, CA Inkson, MC Embree, W Sonoyama, L Li, AI Leet, BM Seo, et al. (2007). Identification of tendon stem/progenitor cells and the role of the extracellular matrix in their niche. Nat Med 13:1219–1227.
4. Zhang J and JHC Wang. (2010). Characterization of differential properties of rabbit tendon stem cells and tenocytes. BMC Musculoskelet Disord 11:10.
5. Rui YF, PPY Lui, G Li, SC Fu, YW Lee and YM Chan. (2010). Isolation and characterization of multi-potent rat tendon-derived stem cells. Tissue Eng Part A 16:1549–1558.
6. Lovati AB, B Corradetti, A Lange Consiglio, C Recordati, E Bonacina, D Bizzaro and F Cremonesi. (2011). Characterization

and differentiation of equine tendon-derived progenitor cells. J Biol Regul Homeost Agents 25(2 Suppl):S75–S84.
7. Shi S and S Gronthos. (2003). Perivascular niche of postnatal mesenchymal stem cells in human bone marrow and dental pulp. J Bone Miner Res 18:696–704.
8. da Silva Meirelles L, PC Chagastelles and NB Nardi. (2006). Mesenchymal stem cells reside in virtually all post-natal organs and tissues. J Cell Sci 119(Pt 11):2204–2213.
9. Crisan M, S Yap, L Casteilla, CW Chen, M Corselli, TS Park, G Andriolo, B Sun, B Zheng, et al. (2008). A perivascular origin for mesenchymal stem cells in multiple human organs. Cell Stem Cell 3:301–313.
10. Zannettino AC, S Paton, A Arthur, F Khor, S Itescu, JM Gimble and S Gronthos. (2008). Multipotential human adipose-derived stromal stem cells exhibit a perivascular phenotype *in vitro* and *in vivo*. J Cell Physiol 214:413–421.
11. da Silva Meirelles L, AI Caplan and NB Nardi. (2008). In search of the *in vivo* identity of mesenchymal stem cells. Stem Cells 26:2287–2299.
12. Caplan AI. (2008). All MSCs are pericytes? Cell Stem Cell 3:229–230.
13. Tempfer H, A Wagner, R Gehwolf, C Lehner, M Tauber, H Resch and HC Bauer. (2009). Perivascular cells of the supraspinatus tendon express both tendon- and stem cell-related markers. Histochem Cell Biol 131:733–741.
14. Theobald P, M Benjamin, L Nokes and N Pugh. (2005). Review of the vascularization of the human Achilles tendon. Injury 36:1267–1272.
15. Lee WYW, PPY Lui and YF Rui. (2012). Hypoxia mediated efficient expansion of human tendon-derived stem cells (hTDSCs) *in vitro*. Tissue Eng Part A 18:484–498.
16. Kurth TB, F Dell'Accio, V Crouch, A Augello, PT Sharpe and C De Bari. (2011). Functional mesenchymal stem cell niches in adult mouse knee joint synovium *in vivo*. Arthritis Rheum 63:1289–1300.
17. Blanpain C and E Fuchs. (2006). Epidermal stem cells of the skin. Annu Rev Cell Dev Biol 22:339–373.
18. Cairns J. (1975). Mutation selection and the natural history of cancer. Nature 255:197–200.
19. Potten CS, G Owen and D Booth. (2002). Intestinal stem cells protect their genome by selective segregation of template DNA strands. J Cell Sci 115(Pt 11):2381–2388.
20. Iwasaki K, M Komaki, N Yokoyama, Y Tanaka, A Taki, Y Kimura, M Takeda, S Oda, Y Izumi and I Morita. (2012). Periodontal ligament stem cells possess the characteristics of pericytes. J Periodontol doi:10.1902/jop.2012.120547.
21. Ni M, PP Lui, YF Rui, YW Lee, YW Lee, Q Tan, YM Wong, SK Kong, PM Lau, G Li and KM Chan. (2012). Tendon-derived stem cells (TDSCs) promote tendon repair in a rat patellar tendon window defect model. J Orthop Res 30:613–619.
22. Rui YF, PPY Lui, M Ni, LS Chan, YW Lee and KM Chan. (2011). Mechanical loading increased BMP-2 expression which promoted osteogenic differentiation of tendon-derived stem cells. J Orthop Res 29:390–396.
23. Mienaltowski MJ, SM Adams and DE Birk. (2013). Regional differences in stem cell/progenitor cell populations from the mouse Achilles tendon. Tissue Eng Part A 19:199–210.
24. Feng J, A Mantesso, C De Bari, A Nishiyama and PT Sharpe. (2011). Dual origin of mesenchymal stem cells contributing to organ growth and repair. Proc Natl Acad Sci U S A 108:6503–6508.
25. Voleti PB, MR Buckley and LJ Soslowsky. (2012). Tendon healing: repair and regeneration. Annu Rev Biomed Eng 14:47–71.
26. Lui PP, YC Cheuk, YW Lee and KM Chan. (2012). Ectopic chondro-ossification and erroneous extracellular matrix deposition in a tendon window injury model. J Orthop Res 30:37–46.
27. Chan BP, SC Fu, L Qin, C Rolf and KM Chan. (1998). Pyridinoline in relation to ultimate stress of the patellar tendon during healing: an animal study. J Orthop Res 16:597–603.
28. Pierantozzi E, B Gava, I Manini, F Roviello, G Marotta, M Chiavarelli and V Sorrentino. (2011). Pluripotency regulators in human mesenchymal stem cells: expression of NANOG but not of OCT-4 and SOX-2. Stem Cells Dev 20:915–923.
29. Arnold K, A Sarkar, MA Yram, JM Polo, R Bronson, S Sengupta, M Seandel, N Geijsen and K Hochedlinger. (2011). Sox2(+) adult stem and progenitor cells are important for tissue regeneration and survival of mice. Cell Stem Cell 9:317–329.
30. Kafienah W, S Mistry, C Williams and AP Hollander. (2006). Nucleostemin is a marker of proliferating stromal stem cells in adult human bone marrow. Stem Cells 24:1113–1120.
31. Jung JS, MK Jee, HT Cho, JI Choi, YB Im, OH Kwon and SK Kang. (2013). MBD6 is a direct target of Oct4 and controls the stemness and differentiation of adipose tissue-derived stem cells. Cell Mol Life Sci 70:711–728.
32. Wang Z and X Yan. (2013). CD146, a multi-functional molecule beyond adhesion. Cancer Lett 330:150–162.
33. Fong G, LJ Backman, G Andersson, A Scott and P Danielson. (2013). Human tenocytes are stimulated to proliferate by acetylcholine through an EGFR signaling pathway. Cell Tissue Res 351:465–475.
34. Hasegawa A, H Nakahara, M Kinoshita, H Asahara, J Koziol and MK Lotz. (2013). Cellular and extracellular matrix changes in anterior cruciate ligaments during human knee aging and osteoarthritis. Arthritis Res Ther 15:R29.
35. Abe H, T Tominaga, T Matsubara, N Abe, S Kishi, K Nagai, T Murakami, T Araoka and T Doi. (2012). Scleraxis modulates bone morphogenetic protein 4 (BMP4)-Smad1 protein-smooth muscle α-actin (SMA) signal transduction in diabetic nephropathy. J Biol Chem 287:20430–20442.
36. Gu TT, SY Liu and PS Zheng. (2012). Cytoplasmic NANOG-positive stromal cells promote human cervical cancer progression. Am J Pathol 181:652–661.
37. Remaud S, SA Lopez-Juarez, AL Bolcato-Bellemin, P Neuberg, F Stock, ME Bonnet, R Ghaddab, MS Clerget-Froidevaux, J Pierre-Simons, et al. (2013). Inhibition of Sox2 expression in the adult neural stem cell niche in vivo by monocationic-based siRNA delivery. Mol Ther Nucleic Acids 2:e89.
38. Dominici M, K Le Blanc, I Mueller, I Slaper-Cortenbach, FC Marini, DS Krause, RJ Deans, A Keating, DJ Prockop and EM Horwitz. (2006). Minimal criteria for defining multipotent mesenchymal stromal cells. The International Society for Cellular Therapy position statement. Cytotherapy 8: 315–317.
39. Halfon S, N Abramov, B Grinblat and I Ginis. (2011). Markers distinguishing mesenchymal stem cells from fibroblasts are downregulated with passaging. Stem Cells Dev 20:53–66.
40. Alt E, Y Yan, S Gehmert, YH Song, A Altman, S Gehmert, D Vykoukal and X Bai. (2011). Fibroblasts share mesenchymal phenotypes with stem cells, but lack their differentiation and colony-forming potential. Biol Cell 103:197–208.
41. Kundrotas G. (2012). Surface markers distinguishing mesenchymal cells from fibroblasts. Acta Medica Lituanica 19:75–79.

42. Schipani E and HM Kronenberg. Adult mesenchymal stem cells. Jan 31, 2009. In: StemBook [Internet]. Cambridge (MA): Harvard Stem Cell Institute; 2008-. Available from: www.ncbi.nlm.nih.gov/books/NBK27056/
43. Nombela-Arrieta C, J Ritz and LE Silberstein. (2011). The elusive nature and function of mesenchymal stem cells. Nat Rev Mol Cell Biol 12:126–131.
44. Rui YF, PPY Lui, G Li, SC Fu, YW Lee and YM Chan. (2010). Isolation and characterization of multi-potent rat tendon-derived stem cells. Tissue Eng Part A 16:1549–1558.
45. Lui PPY. (2013). Identity of tendon stem cells—how much do we much? J Cell Mol Med 17:55–64.

Address correspondence to:
Dr. Pauline Po Yee
9/F, Rumsey Street, Multi-Storey Carpark Building
2 Rumsey Street, Sheung Wan
Hong Kong SAR
China

E-mail: paulinelui00@gmail.com

Received for publication February 2, 2013
Accepted after revision July 1, 2013
Prepublished on Liebert Instant Online July 1, 2013